UNBRANCHED3 regulates branching by modulating cytokinin biosynthesis and signaling in maize and rice

Yanfang Du[1], Lei Liu[1], Manfei Li[1], Shuang Fang[2], Xiaomeng Shen[1], Jinfang Chu[2] and Zuxin Zhang[1,3]

[1]Key Laboratory of Crop Genetic Improvement, Huazhong Agricultural University, Wuhan 430070, China; [2]National Centre for Plant Gene Research (Beijing), Institute of Genetics and Developmental Biology, Chinese Academy of Sciences, Beijing 100049, China; [3]Hubei Collaborative Innovation Center for Grain Crops, Jingzhou 434025, China

Author for correspondence:
Zuxin Zhang
Tel: +86 027 87282689
Email: zuxinzhang@mail.hzau.edu.cn

Summary

• *UNBRANCHED3* (*UB3*), a member of the SQUAMOSA promoter binding protein-like (*SPL*) gene family, regulates kernel row number by negatively modulating the size of the inflorescence meristem in maize. However, the regulatory pathway by which *UB3* mediates branching remains unknown.

• We introduced the *UB3* into rice and maize to reveal its effects in the two crop plants, respectively. Furthermore, we performed transcriptome sequencing and protein-DNA binding assay to elucidate the regulatory pathway of *UB3*.

• We found that *UB3* could bind and regulate the promoters of *LONELY GUY1* (*LOG1*) and Type-A response regulators (*ARRs*), which participate in cytokinin biosynthesis and signaling. Overexpression of exogenous *UB3* in rice (*Oryza sativa*) dramatically suppressed tillering and panicle branching as a result of a greater decrease in the amount of active cytokinin. By contrast, moderate expression of *UB3* suppressed tillering slightly, but promoted panicle branching by cooperating with *SPL* genes, resulting in a higher grain number per panicle in rice. In maize (*Zea mays*) *ub3* mutant with an increased kernel row number, *UB3* showed a low expression but cytokinin biosynthesis-related genes were up-regulated and degradation-related genes were down-regulated.

• These results suggest that *UB3* regulates vegetative and reproductive branching by modulating cytokinin biosynthesis and signaling in maize and rice.

Introduction

The branches of rice (*Oryza sativa* L.) and maize (*Zea mays* L.) are composed of tillers produced from axillary meristems (AMs) and inflorescence branches produced from branch meristems (BMs). Upon the transition from the vegetative to the reproductive phase, the shoot apical meristem (SAM) is converted into the inflorescence meristem (IM), which is responsible for the production of the panicle in rice or the tassel in maize, both of which typically exhibit a few long branches. In rice, the axillary SAMs of the tillers also transit into the IMs and develop into the panicle. Unlike rice, the axillary SAM in the axil of maize leaves becomes a female inflorescence meristem that develops into ear branches (Vollbrecht & Schmidt, 2009). Thus, the meristem transition and the determination of distinct axillary meristems play important roles in the branching patterns of rice and maize, controlled by complex and conserved networks, including the *CLAVATA* (*CLV*)-*WUSCHEL* (*WUS*) negative feedback loop, the *KNOX* pathway, small RNA-mediated gene silencing and hormone signaling (Ha *et al.*, 2010; Pautler *et al.*, 2013). In rice, the *CLV*-like genes *floral organ number1* (*fon1*) and *fon2* (Suzaki *et al.*, 2004, 2006) and the CLE domain-encoding genes *FON2-LIKE CLE PROTEIN1* (*FCP1*) and

FCP2 (Suzaki *et al.*, 2008, 2009) are involved in the maintenance of SAMs and the floral meristem. *WUSCHEL-RELATED HOMEOBOX4* (*WOX4*) is negatively regulated by *FCP1*, and it is also involved in the maintenance of the SAM by regulating the expression of *homeobox1* (*OSH1)* and *FON2* (Ohmori *et al.*, 2013). The WUS-like gene *TAB 1* is expressed in the premeristem zone and promotes the formation of the axillary meristem by up-regulating *OSH1* (Tanaka *et al.*, 2015). In addition, the *KNOX* genes *OSH1* and *OSH15* are indispensable for the establishment and maintenance of the SAM and floral meristem, and also regulate the cytokinin signaling pathway (Tsuda *et al.*, 2011, 2014). There is increasing evidence that phytohormones play crucial roles in modulating the initiation and maintenance of meristems (Pautler *et al.*, 2013). Auxin is typically synthesized in the shoot apex in young leaves and is subsequently transported basipetally via the polar transport stream to control bud activation and outgrowth. By contrast, cytokinins are exported from the roots to the AM through the xylem system, promoting bud activation (Müller & Leyser, 2011). Strigolactones (SLs), a novel inhibitor of AM outgrowth, may act downstream of auxin or independently of polar auxin transport (Gomez-Roldan *et al.*, 2008). Moreover, microRNAs and their targeted transcription factors participate in regulating the rice tillering and branching

system. The optimal panicle size of rice is regulated by the fine-tuned regulatory pathway of *MicroRNA156* (*miR156*)/*miR529*/*SQUAMOSA PROMOTER BINDING PROTEIN LIKE* (*SPL*). *MiR172/APETALA2* (*AP2*) also regulates the spikelet transition without affecting tillering (Wang *et al.*, 2015).

In maize, *TEOSINTE BRANCHED1* (*TB1*) acts as a repressor of the axillary organ, leading to a drastic decrease in branches in modern maize relative to its progenitor teosinte (Studer *et al.*, 2011). The *CLV-WUS* pathway is conserved in rice and maize (Pautler *et al.*, 2013), and mutations of *CLV-WUS* pathway genes, such as *THICK TASSEL DWARF1* (*TD1*), *FASCIATED EAR2* (*FEA2*), *FASCIATED EAR3* (*FEA3*) and *COMPACT PLANT2* (*CT2*), lead to enlarged IMs, fasciated ears, and extra kernel rows (Bommert *et al.*, 2005, 2013a,b; Je *et al.*, 2016). A b-ZIP transcription factor, *FASCIATED EAR4* (*FEA4*), also modulates the size of the SAM and IM by regulating auxin signaling, acting in parallel to the canonical *CLV-WUS* pathway (Pautler *et al.*, 2015). In addition to *FEA4*, *BARREN INFLORESCENCE1* (*BIF1*) and *BIF4*, which encode auxin/IAA (Aux/IAA) proteins, function in establishing critical boundary domains to ensure the formation of new axillary meristems that subsequently develop into branches and spikelets (Galli *et al.*, 2015). Both *Corngrass1* (*Cg1*), encoding two tandem *miR156* genes, and *Tasselseed4* (*ts4*), encoding *miR172*, are involved in regulating the phase transition, identity and determinacy of axillary meristems via small RNA-mediated gene silencing pathways (Chuck *et al.*, 2007a,b). In addition, three genes, *RAMOSA1* (*RA1*), *RA2* and *RA3*, are key regulators of the determinacy of branch meristems and spikelets pair meristems via interactions with *KNOTTED1* to promote hormone biosynthesis and signaling (Tanaka *et al.*, 2013; Eveland *et al.*, 2014). Thus, the maize and rice branching pattern are regulated by conserved genes and pathways.

UNBRANCHED3 (*UB3*), is an ortholog of *OsSPL14* which directly regulates *OsTB1* and *DENSE AND ERECT PANICLE1* (*DEP1*) to repress rice tillering and to activate spikelet meristems (Jiao *et al.*, 2010; Miura *et al.*, 2010; Lu *et al.*, 2013). *UB3* regulates the determinacy of the axillary meristem of maize (Chuck *et al.*, 2014), and a recent study has revealed that *UB3* is controlled by *KRN4*, a closely linked quantitative trait locus for kernel row number (KRN), and that expression level of *UB3* is negatively correlated with KRN (Liu *et al.*, 2015). However, the molecular mechanism by which *UB3* represses KRN remains unknown. Here, we introduced *UB3* into maize and rice to reveal the effects of its overexpression in the two crop plants, respectively. Furthermore, we integrated transcriptome data from the shoot apices and young panicles collected from highly expressing *UB3* transgenic rice plants and the available ChIP-Seq data (Lu *et al.*, 2013) to identify potential genes bound by *UB3*. We subsequently validated *UB3* binding sites using electrophoresis mobility shift assays. The candidate pathways identified in rice for the regulation of branching were assayed in a maize *ub3* mutant. We found a shared pathway of *UB3* that regulates the vegetative and reproductive branches in rice and maize by modulating the cytokinin level and signaling.

Materials and Methods

Maize and rice genetic transformation

For maize (*Zea mays* L.) genetic transformation, the *UB3* coding sequence with a mutated *miR156* target site fused to yellow fluorescent protein (YFP) was cloned into the *pCAMBIA3301* vector, in which the *CaMV35S* promoter was replaced with the *ubiquitin* promoter to produce *pUbi::UB3+YFP*. The mutated *miR156* target sites were the 847th (T-C), 858th (T-G), and 867th (A-C) nucleotides of the *UB3* CDS, which are located on the second, 11th and 20th positions of *miR156*, respectively. The binary expression vector was transformed into the *Agrobacterium tumefaciens* strain *EHA105*, which was then coincubated with immature embryos of the maize inbred line A188 (Frame *et al.*, 2002). After 3 d of coincubation, all embryos were transferred to subculture. After 2 months, the calli were assessed for the presence of YFP, screened by gradient concentration of hygromycin and then amplified using specific primers (Supporting Information Table S1) derived from the *ubiquitin* promoter and *UB3* sequence. Positive calli were transferred into regeneration medium. The T_0-regenerated seedlings were cultivated in a glasshouse at 30°C (day) and 25°C (night) with 16 : 8 h, light : dark. Those transgenic individuals were re-examined using specific primers (Table S1) to detect positive transgenic individuals. Those individuals with a *UB3* insertion and a high expression level of *UB3* were then identified by Southern blotting using digoxigenin (DIG)-labeled probes (primers listed in Table S1), which were synthesized using the DNA probe label with the DIG DNA Labeling kit (#11175033910, Roche). All Southern-positive transgenic individuals were used for phenotypic evaluation. All nontransgenic maize individuals (A188-NT) were used as controls.

For rice (*Oryza sativa* L.) genetic transformation, the *UB3* coding sequence with the mutated *miR156* target site equipped with the *CaMV-35S* promoter was inserted into the *pCAMBIA1300* vector to produce the *p35S::UB3* construct, which was then introduced into a japonica rice variety, 'Nipponbare'. T_0 or T_1 plants were cultivated in a glasshouse. A pair of primers derived from the *CaMV35S* promoter and *UB3* sequence was used to detect transgenic individuals. The *UB3* expression in each T_0 or T_1 individual was also analysed by reverse transcription polymerase chain reaction (RT-PCR) using the primers listed in Table S1. Those progeny plants derived from T_0 nontransgenic rice individuals were used as controls (UB3-NT).

Measurement of endogenous cytokinin

A total of 0.5 g of shoots was separately collected from seedlings of UB3-OE(54/78) and UB3-NT grown for 60 d after germination, with three biological replicates. Cytokinin, including trans-zeatin (tZ), dihydrozeatin (DZ), trans-zeatin riboside (tZR), isopentenyladenine (iP) and isopentenyladenosine (iPR), were measured at the National Centre for Plant Gene Research (Beijing), Institute of Genetics and

Developmental Biology, Chinese Academy of Sciences (Beijing, China). Fresh plant tissues were frozen in liquid nitrogen and homogenized to fine powder using a ball mill Retsch MM 400 (Retsch, Newtown, PA, USA) at a frequency of 30 Hz for 1 min. Around 400 mg of ground powder was extracted for 24 h in extraction solvent (methanol/water/formic: 15/4/1, v/v/v) with the internal standards of [2H5]tZ, [2H5]tZR, [2H5] DHZ, [2H6]iP, [2H6]iPR (400 pg, OlChemIm) added. The supernatant was centrifuged for 15 min at 15 000 g and dried with nitrogen stream and then dissolved in 2 ml of formic acid (2 mol l^{-1}). Crude extracts were further purified by loading onto the Oasis MCX cartridge (500 mg 6^{-1} ml; Waters, Milford, MA, USA) preconditioned with 4 ml of methanol, water and formic acid (2 mol l^{-1}). The cartridge was sequentially washed with formic acid (1 mol l^{-1}), formic acid (0.5 mol l^{-1}), formic acid (0.5 mol l^{-1}) in 60% methanol, water, 5% methanol, ammonia solution (0.5 mol l^{-1}) in 5% methanol, ammonia (0.4 mol l^{-1}), formic acid (2 mol l^{-1}) and methanol. Cytokinins were eluted with 4 ml of 5% ammonia in methanol and dried with nitrogen gas. Dried elution was dissolved in 50% methanol for analysis on a LC–tandem MS system consisting of an Acquity UPLC (Waters) and Qtrap 5500 system (AB Sciex, Shinagawa-ku, Tokyo, Japan) equipped with Electron Spray Ionization source.

The separation was achieved on an Acquity UPLCTM BEH C18 column (100 mm × 2.1 mm, 1.7 μM; Waters) with the column temperature set at 30°C and the flow rate at 0.5 ml min^{-1}. The 8.5 min linear gradient runs from 98% to 75% A (solvent A, 0.05% acetic acid in water; solvent B, 0.05% acetic acid in acetonitrile) in 5.0 min, 75–20% A in the next 0.5 min and is returned to the initial condition for 3 min for equilibration. Cytokinins were detected in positive MRM mode and the source parameters were set as follows: ion spray voltage, 5300 V; desolvation temperature, 600°C; nebulizing gas 1, 45; desolvation gas 2, 60; and curtain gas, 30. The MRM transitions for cytokinins were as follows: 220.1 > 136.0 (tZ), 352.2 > 220.1 (tZR), 222.1 > 136.0 (DHZ), 204.1 > 136.0 (iP), and 336.1 > 204.1 (iPR).

Real-time PCR

To analyze expression of *UB3* in transgenic maize and rice plants, *c.* 1.0 g of samples were collected from the leaves of each T$_0$-regenerated maize seedling after 4 wk of growth in the glasshouse, and from the leaves of each 4-wk-old T$_1$ transgenic rice and UB3-NT. In addition, young panicles (YPs) of T$_2$ individuals at 4 wk after transplanting were collected from the moderate *UB3* expression line UB3-OE(30). Total RNA was extracted using TRIzol$^®$ reagent (Life Technologies, Invitrogen) according to the user manual. The EasyScript one-step gDNA-removal and cDNA-Synthesis Supermix Kit (Transgene, Beijing, China) was used for cDNA synthesis, and SBRY Green PCR Master Mix (Transgene) was used for amplification with the Bio-Rad CFX96 real-time PCR detection system using gene-specific primer pairs (Table S1). The expression levels were normalized to *ACTIN1* (*LOC_Os10g36650*) in rice or *ACTIN* (*GRMZM2G126010*) in maize.

Transcriptome sequencing

Two rice transgenic T$_1$ lines, UB3-OE(54) and UB3-OE(78), and UB3-NT were used for transcriptome sequencing. Approximately 1.0 g of sample was collected separately from the shoot apices (SAs) of individuals at 2 wk after transplanting, and from young YPs of individuals at 4 wk after transplanting. The samples from the two transgenic lines of the same tissue were pooled for total RNA isolation with three biological replicates. Additionally, *c.* 1.0 g of sample was collected separately from an immature ear (5–8 mm) of the *ub3::mum* and W22 (wild-type) in maize with three biological replicates. Total RNAs were isolated using TRIzol$^®$ reagent (Life Technologies, Invitrogen). Construction of the cDNA library and sequencing were performed at the Beijing Genomics Institute (BGI, Shenzhen, China) using the Illumina system HiSeq2500 (Illumina Inc., San Diego, CA, USA). The raw reads were preprocessed using the FASTX-Toolkit to generate high-quality clean reads (Goecks *et al.*, 2010). The FastQC program was used to assess the quality of the clean reads (Andrews, 2010), which were then aligned to the rice reference genome Release 7 of the MSU Rice Genome Annotation Project using TOPHAT v.2.1.0 (Trapnell *et al.*, 2012). CUFFLINKS v.2.1.1 (Trapnell *et al.*, 2012) was then used to normalize and estimate the gene expression level according to fragments per kilobase of transcript per million reads (FPKM; Mortazavi *et al.*, 2008). The differentially expressed genes (DEGs) were also calculated using CUFFLINKS v.2.1.1 at a significance level of $P < 0.01$. All RNA samples for transcriptome sequencing were also used to validate the expression level of the DEGs.

Electrophoretic mobility shift assay (EMSA)

The full-length UB3 coding sequence was inserted into the expression vector *pGEX 4T-1*. The expression of the fusion protein UB3-GST was induced in *BL21*-transfected cells (Transgene) in the presence of 0.2 mM isopropyl-1-thio-D-galactopyranoside at 37°C for 3 h, and the expressed fusion protein was then purified using glutathione S-transferase (GST) Sefinose Resin (Sangon Biotech, Shanghai, China) and quantified using the Sangon Biotech protein assay reagent following the manufacturer's protocols and sodium dodecyl sulfate–polyacrylamide gel electrophoresis (PAGE). The EMSA assay was performed using EMSA Kit (LightShift$^®$ Chemiluminescent EMSA Kit and Chemiluminescent Nucleic Acid Detection Module, Thermo Scientific, Waltham, MA, USA). The single-stranded DNA probe (50–60 bp) was synthesized with a 5′-end biotin label (Table S2) and dissolved in ddH$_2$O to a final concentration of 5 μM. Approximately 5 μl of forward DNA probe was mixed with 5 μl of reverse DNA probe. The mixed probes were incubated at 100°C for 5 min and then slowly cooled at room temperature to anneal into double-stranded probes. The labeled double-strand DNA probes were then diluted to 100 fM, and the unlabeled DNA probes were diluted to 2 pM. The labeled and unlabeled probes (2 μl of each) were incubated with purified proteins (20–40 ng fusion protein per reaction) in 20 μl mixtures containing 9 μl of ultrapure water, 2 μl of 10 × binding buffer

(100 mM Tris, 500 mM KCL,10 mM dithiothreitol; pH 7.5), 1 µl of 50% glycerol, 1 µl of 100 mM $MgCl_2$, 1 µl of poly (dI-dC) (1 µg µl^{-1} in 10 mM Tris,1 mM ethylenediaminetetraacetic acid (EDTA), pH 7.5), and 1 µl of 1% NP-40 at room temperature for 20 min. After the addition of 5 µl of 5 × loading buffer, the samples were subjected to electrophoresis on 6% nondenaturing PAGE gels in 0.5 × Tris-Borate-EDTA buffer (0.045 mol l^{-1} Tris-Borate, 1 mmol l^{-1} EDTA, pH 8.0) at 100 V and 4°C for 1 h. The binding reactions were then transferred to a nylon membrane at 380 mA (~ 100 V) for 45 min at 4°C in 0.5× Tris-borate-EDTA buffer. Following transfer, the membrane was crosslinked to the transferred DNA at 80°C for 2 h. The membrane was visualized by chemiluminescence.

Results

UB3 represses maize calli regeneration

UB3 is a negative regulator of maize KRN (Chuck *et al.*, 2014; Liu *et al.*, 2015). To reveal the underlying mechanism, we over-expressed *UB3* with a mutated *miR156* target site in maize via *Agrobacterium tumefaciens*-mediated transformation (Frame *et al.*, 2002). The *UB3*-encoding DNA sequence fused to a YFP tag was driven by the *Ubiquitin* promoter (*pUbi::UB3-YFP*). Positive calli were selected by screening with a gradient concentration of hygromycin, amplifying the target gene, and visualizing the YFP. A total of 576 positive calli clones were selected for subculturing, but after 3 wk, 508 clones (87.8%) started to become brown relative to the negative calli (Fig. 1a,b), and they were difficult to regenerate into seedlings (Fig. 1c). The remaining calli differentiated into three types of seedlings, UB3-OE1 (*UB3* overexpression 1), UB3-OE2 and UB3-OE3. Southern blot showed that the *pUbi::UB3-YFP* was inserted as a single copy into the genome of the three types of seedlings (Fig. 1e). Quantitative real-time PCR (QRT-PCR) showed that the expression levels of *UB3* were 3.6-, 3.5- and 1.9-fold higher in the leaves of UB3-OE1, UB3-OE2 and UB3-OE3 transgenic seedlings, respectively, compared with that of endogenous *UB3* in nontransgenic plants (A188-NT) (Fig. 1f). However, after transplantation into the glasshouse, the growth of all three types of seedlings was compromised, and both shoot and root growth were strongly suppressed (Fig. 1c,d).

Effects of UB3 on tillering and panicle branching in rice

Because of the failure of *UB3* overexpression in maize, we introduced the mutated maize *UB3* into Nipponbare (Japonica rice) and obtained six independent transgenic events. We measured *UB3* expression level of leaves of all individuals in each T_1 family using QRT-PCR. Based on the expression level of *UB3*, the six *UB3* overexpression lines could be divided into two groups. Two lines, UB3-OE(78) and UB3-OE(54), displayed a very high expression level of *UB3*, which was 10-fold higher (referred to as high *UB3* expression) than that in UB3-NT (Fig. 2b). The two lines have few tillers and short panicles, suggesting that high levels of *UB3* suppressed plant tillering and panicle branching (Fig. 2a,c,i–l; Table S3). The initiation rates of the leaves was not significantly different during the vegetative stage; however, the tiller buds were produced later and grew more slowly in these two lines than in UB3-NT plants. Also plant heights of UB3-OE (78) and UB3-OE(54) were lower and the heading date was later than those of UB3-NT (Fig. 2a,f–h; Tables S3, S4). For example, the average plant heights of UB3-OE(78) and UB3-OE(54) were 60.48 and 52.67 cm, respectively, which were significantly lower than the average height of UB3-NT (83.83 cm). The panicle lengths of UB3-OE(78) (14.52 cm) and UB3-OE(54)
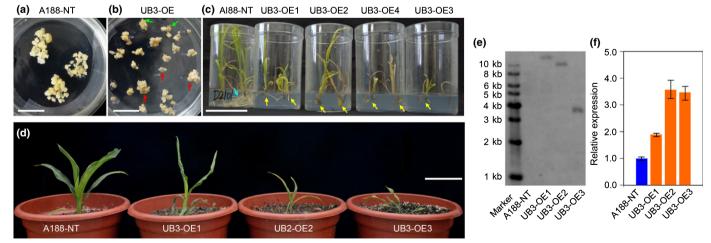

Fig. 1 Performance of *UB3*-overexpressing maize lines and nontransgenic plants. (a) Calli of the wild-type after 2 months of subculture. Bar, 3 cm. (b) Positive calli with high *UB3* expression after 1 month of subculture. Green and red arrows indicate regeneration seedlings and brown calli, respectively. Bar, 10 cm. (c) Regeneration seedlings of different transformation events (2 months). The blue arrow shows the robust roots of nontransgenic seedlings (A188-NT referred to *UB3* nontransgenic plants in maize), and the yellow arrows show the few and weakened roots of the transgenic seedlings of UB3-OE lines. Bar, 10 cm. (d) Transplanted transgenic seedlings of different transformation events. Bar, 10 cm. (e) Southern blotting of three transformation events. (f) The relative expression level of *UB3* in the young leaves of nontransgenic (A188-NT) and transgenic seedlings. *ACTIN* (*GRMZM2G126010*) was used as the internal control. Error bars represent ± SE (*n* = 3).
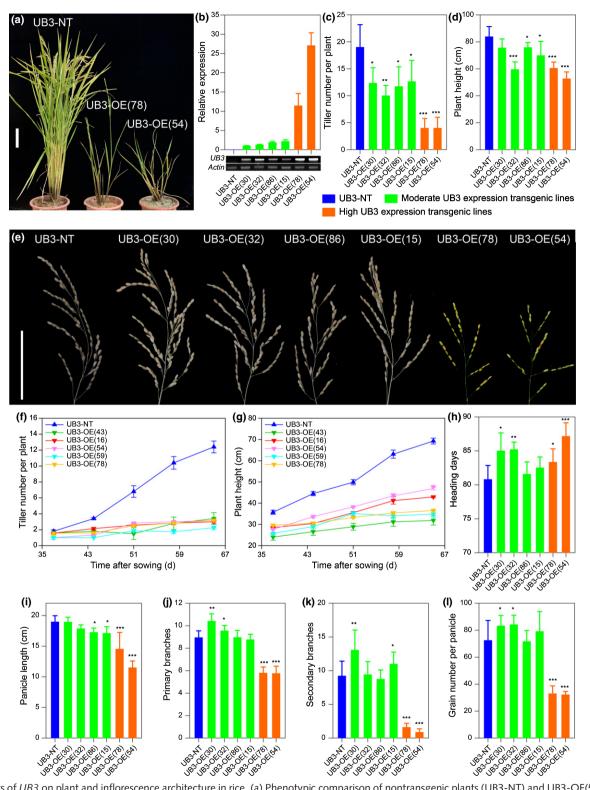
Fig. 2 Effects of *UB3* on plant and inflorescence architecture in rice. (a) Phenotypic comparison of nontransgenic plants (UB3-NT) and UB3-OE(54) and UB3-OE(78) in the T$_1$ generation (3 months after transplanting). Bar, 10 cm. (b) The relative expression levels of *UB3* in the leaves of different transformation events (2 wk after transplanting). Rice *Actin1* (*LOC_Os10g36650*) was used as the internal control. Values are means ± SE (*n* = 3). (c) Statistical comparisons of tillers, (d) plant height, (h) heading days, (i) panicle length, (j) primary branch, (k) secondary branch and (l) grains per panicle at 100 d after sowing in UB3-NT and *UB3* overexpression lines. (e) The mature panicles of UB3-NT and *UB3* overexpression lines. The panicle in the moderate *UB3* expression line UB3-OE(30) is larger than that of UB3-NT, and the panicles in the high *UB3* expression lines UB3-OE(78) and UB3-OE(54) are smaller than that of UB3-NT Bar, 10 cm. (f, g) The dynamic changes of (f) tiller, and (g) plant height in five *UB3* transgenic rice lines. The statistical significance was estimated by a Student's *t*-test (*n* > 5). *, *P* < 0.05; **, *P* < 0.01; ***, *P* < 0.001. Error bars represent ± SD. Blue columns, UB3-NT; green columns, *UB3* moderate expression lines; red columns, *UB3* high expression lines.

(11.49 cm) were shorter than that of UB3-NT (18.95 cm) as well (Fig. 2i; Table S3). Similarly, the tiller number per plant in the two lines (4.00 for both) was significantly less than that in UB3-NT (19.00) (Fig. 2c,d; Table S3). The primary and secondary inflorescence branches were significantly repressed in UB3-OE (78) and UB3-OE(54) (only 65% and 17% of UB3-NT plants, respectively; Fig. 2j,k; Table S3). The average grain numbers per panicle in UB3-OE(78) and UB3-OE(54) were 32.92 and 32.17, respectively, which are only 45% and 44% of that in UB3-NT plants, and most grains were filled incompletely at the mature stage (Fig. 2e,l; Table S3). These results demonstrated that higher expression of *UB3* altered the branching pattern of rice, resulting in strong suppression of tillering and panicle branching and a delay of the transition from the vegetative to the reproductive stage. The expression of *UB3* in the second type of transgenic plants was one- to three-fold higher (referred to as moderate *UB3* expression) than *ACTIN1* in UB3-NT. This type included four transgenic lines, UB3-OE(15), UB3-OE(30), UB3-OE(32) and UB3-OE(86) (Fig. 2b). Compared with UB3-NT, the primary and secondary panicle branches in UB3-OE(30) grew significantly more, and tiller number and plant height were slightly reduced (Fig. 2c–e,i–l; Table S3).

Furthermore, we analyzed the expression level of *UB3* and three other endogenous genes, including *OsSPL7*, *OsSPL14* and *OsSPL17*, in the YPs, and found that *OsSPL7*, *OsSPL14* and *OsSPL17* were down-regulated in UB3-OE(54/78) with high *UB3* expression but up-regulated in UB3-OE(30) with moderate *UB3* expression (Fig. 3a,b). This result indicated that exogenous *UB3* expression at an appropriate level (about equal to *Actin1* expression level in UB3-OE(30)) can promote panicle branching by regulating expression of *SPL* genes, which is consistent with
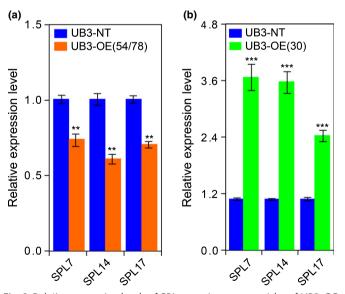
recent study showing that panicle branching depends on the expression level of *SPL* gene (Wang *et al.*, 2015).

Genes regulated by *UB3*

To unravel the regulatory pathway of *UB3* in rice, the SAs and YPs were collected separately from UB3-OE(54/78) and UB3-NT, and the transcriptome of each was sequenced in three biological replicates. A total of 2226 DEGs were found in the SAs of UB3-OE(54/78), with a *P*-value < 0.05 (Fig. 4a; Table S5). Among these genes, 718 were up-regulated and 1508 were down-regulated in SAs of UB3-OE(54/78). Similarly, 2467 DEGs, including 1492 up-regulated genes and 975 down-regulated genes, were found in YPs of UB3-OE(54/78) (Fig. 4a; Table S5). We found that 226 up-regulated and 274 down-regulated genes were shared between SAs and YPs (*P*-value < 0.05) (Fig. 4a). Moreover, 24 DEGs were up-regulated in SAs but down-regulated in YPs, while 150 DEGs were down-regulated in SAs but up-regulated in YPs (Fig. 4a).

These DEGs were involved in a wide spectrum of biological processes and metabolic pathways, or containing different transcription factor families (Fig. 4b–f). Gene ontology analysis showed that DEGs in SAs and YPs were most enriched in biological processes that respond to abiotic stimulus and stress, had a molecular function related to transcription regulator activity, and acted in the extracellular cellular component (*P* < 0.0001) (Fig. 4b). In particular, most of the genes participating in cytokinin biosynthesis and signaling were down-regulated (Figs 4f, S1). *LOG1*, which encodes a cytokinin riboside 5′-monophosphate phosphoribohydrolase (Kurakawa *et al.*, 2007), was repressed in both the SAs and YPs of UB3-OE(54/78), compared with those in the two tissues of UB3-NT (Figs 5b, S1). Additionally, the A-type response regulator genes (*ARRs*), which act as markers for active cytokinin in the SAM (Jain *et al.*, 2006), were also repressed in UB3-OE(54/78) lines. For example, *OsRR1*, *OsRR4* and *OsRR6* were greatly down-regulated in the SAs and both *OsRR9* and *OsRR10* were down-regulated in the YPs of UB3-OE(54/78) (Figs 5d,e, S1). *OsCKX2*, a cytokinin oxidase/dehydrogenase (*CKX*) family gene that negatively regulates SAM activity and seed production (Ashikari *et al.*, 2005), was highly expressed in SAs of UB3-OE (54/78) (Figs 5c, S1), suggesting a rapid degradation of cytokinin in the SAs of UB3-OE(54/78). All of these results suggest that bioactive cytokinin in SAs and YPs of UB3-OE (54/78) were lower than those in the two tissues of UB3-NT (Figs 4f, S1). To test this hypothesis, we measured the concentrations of cytokinin in 60-d-old shoots of UB3-OE(54/78) and UB3-NT. The total content of active forms of cytokinin, including tZ and iP, was slightly lower in UB3-OE(54/78) ($10.1 \pm 1.1 \text{ pg g}^{-1}$) than in UB3-NT ($11.9 \pm 0.8 \text{ pg g}^{-1}$) (Student's *t*-test, *P* = 0.034). In particular, the tZ content was significantly lower in UB3-OE(54/78) than in UB3-NT (Student's *t*-test, *P* = 0.0023). However, the contents of the two precursors, tZR (*P* = 0.057) and iPR (*P* = 2.1E–05) in UB3-OE(54/78) were higher than that in UB3-NT. These results indicated that the precursors could not be effectively

Fig. 3 Relative expression levels of *SPL* genes in young panicles of UB3-OE (54/78), UB3-OE(30) and nontransgenic plants (UB3-NT) in rice. (a) Relative expression levels of *SPL7*, *SPL14*, and *SPL17* in the young panicles of UB3-OE(54/78) and UB3-NT. (b) Relative expression levels of *SPL7*, *SPL14*, and *SPL17* in the young panicles of UB3-OE(30) and UB3-NT. Rice *Actin1* was used as the internal control. **, *P* < 0.01; ***, *P* < 0.001. Error bars represent ± SE.
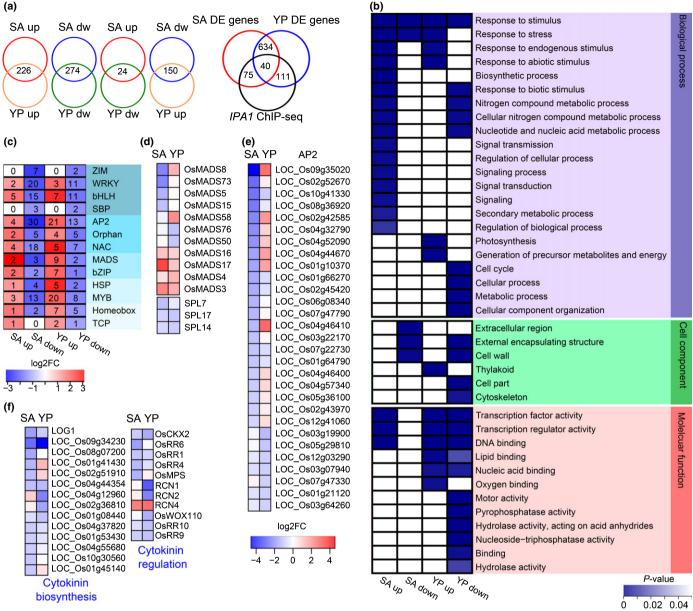
Fig. 4 Transcriptome profiling in UB3-OE(54/78) and the nontransgenic line (UB3-NT) in rice. (a) Overview of differentially expressed genes (DEGs) in shoot apices (SAs) and young panicles (YPs) between UB3-NT and UB3-OE(54/78) and comparison among differentially expressed genes with *IPA1* ChIP-seq data (Supporting Information Table S6). SA up and YP up, DEGs with increasing expression levels in SAs and YPs of UB3-OE(54/78), respectively. SA dw and YP dw, DEGs with decreasing expression levels in SAs and YPs of UB3-OE(54/78), respectively. $P < 0.05$. (b) Gene ontology (GO) enrichment of DEGs for biological processes, cell components and molecular functions. (c) Number of differentially expressed transcription factors and mean of the fold change in UB3-OE(54/78) relative to UB3-NT. (d) Differentially expressed *MADS-box* genes and *SPL* genes. (e) Differentially expressed *AP2* gene family. (f) DEGs in cytokinin biosynthesis and regulation pathway. The color in each cell indicates the value of the log$_2$ fold-change (log$_2$FC). All DEGs are listed in Table S5.

converted into the active forms (tZ and iP) of cytokinins in UB3-OE(54/78) as a result of the lower expression of cytokinin biosynthesis-related genes *LOG1* and *LOC_OS04G44354* (Fig. 6a).

In addition to cytokinins, the concentration of IAA was clearly lower in UB3-OE(54/78) (4.40 ± 0.21 pg mg^{-1}) than in UB3-NT (6.81 ± 0.56 pg mg^{-1}) ($P = 0.0022$) (Fig. S2b). Among the DEGs, many genes associated with auxin biosynthesis and transport were identified as well (Fig. S2a). For example, *Small Auxin-*

up RNA39 (*SAUR39*), a negative regulator of auxin synthesis and transport in rice (Kant *et al.*, 2009), and *OsPIN5b,* a negative regulator of rice plant height, tiller number and panicle length (Lu *et al.*, 2015), were up-regulated in YPs of UB3-OE(54/78) compared with that in UB3-NT (Fig. S2d,e). *RICE FLORICULA/ LEAFY (RFL)*, a positive regulator of the outgrowth of AMs by influencing auxin transport (Deshpande *et al.*, 2015), was down-regulated in both SAs and YPs of UB3-OE(54/78) relative to that in UB3-NT (Fig. S2c). The expression of genes might partly
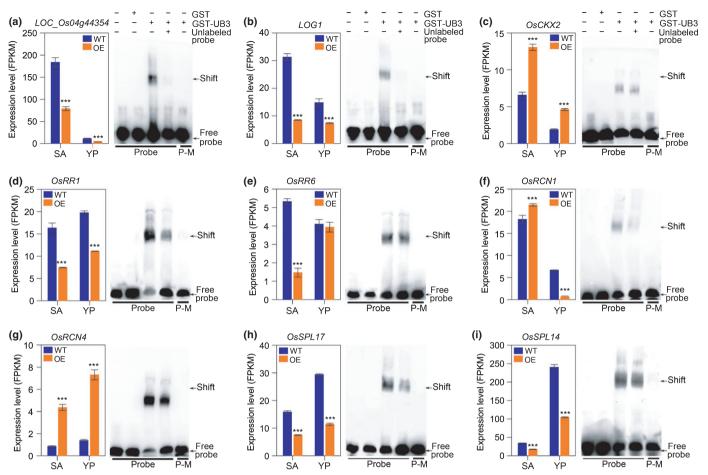
Fig. 5 Putative targets of *UB3* in the regulation of rice tillering and panicle branching. The histogram in the box shows the expression (FPKM value) of genes in transgenic UB3-OE(54/78) and nontransgenic UB3-NT, including (a) *LOC_Os04g44354*, (b) *LOG1*, (c) *OsCKX2*, (d) *OsRR1*, (e) *OsRR6*, (f) *RCN1*, (g) *RCN4*, (h) *SPL14* and (i) *SPL17*. The gel shift images show that UB3 protein binds directly to the promoter regions of these genes containing a GTAC motif according to an electrophoretic mobility shift assay (EMSA). Probe, a 50–60 bp DNA containing the GTAC motif. P-M, the mutant probe with GCAC that serves as the negative control. *, $P < 0.05$; **, $P < 0.01$; ***, $P < 0.001$. Error bars represent $\pm$ SE ($n = 3$) EMSA probe sequences are listed in Supporting Information Table S2. SA, shoot apex; YP, young panicle; FPKM, fragments per kilobase of transcript per million reads.

explain the low concentration of IAA in shoots, and the reduced plant height, tiller number, and panicle length in UB3-OE(54/78).

Many transcription factors (TFs) were also differentially expressed in UB3-OE(54/78) and UB3-NT, especially some inflorescence-related TFs, including *MADS-box*, *AP2* and *SPL* genes (Fig. 4c–e). *MADS-box* genes are bound by *SBP/SPL* TFs to regulate floral organ specification (Bartlett *et al.*, 2015). We detected 11 MADS-box genes that were significantly down- or up-regulated in YPs of UB3-OE(54/78) ($P < 0.0001$) (Fig. 4d). *OsMADS58* was highly expressed in YPs of UB3-OE(54/78) (Figs 4d, S1), and previous studies showed *OsMADS58* interacting with *OsMADS1* to control floral meristem determinacy and suppress spikelet meristem reversion (Hu *et al.*, 2015; Zheng *et al.*, 2015). Twenty-nine AP2 domain-containing genes were differentially expressed, and most of them were down-regulated in both SAs and YPs ($P < 0.0001$) (Fig. 4e). *BRANCHED FLORETLESS 1* (*BFL1*), a member of the *AP2* gene family that functions in the transition from the spikelet to the floral meristem (Zhu *et al.*, 2003), was down-regulated in SAs and up-

regulated in YPs (Figs 4e, S1). Among the *SPL* genes, Os*SPL7*, Os*SPL14* and Os*SPL17*, which positively regulate the activities of inflorescence meristems and branch meristems (Wang *et al.*, 2015), were down-regulated in both SAs and YPs of UB3-OE(54/78) (Figs 4d, 5h,i). The down-regulation of these three *SPL* genes indicated that inflorescence branching might be hindered in UB3-OE(54/78). Furthermore, the *PANICLE PHYTOMER2* (*PAP2*)/*Rice TFL1*/*CEN* homolog gene, *RCN1*, was down-regulated while *RCN4* was up-regulated in YPs of UB3-OE(54/78) (Figs 3f, 5f,g). *RCN1* is positioned downstream of *SPLs* to regulate the transition from the vegetative to the reproductive phase (Wang *et al.*, 2015). Thus, *UB3* might regulate the development of SAs and YPs by the regulation of *AP2/SPL/MADS* to *RCN1/RCN4* directly or indirectly.

Direct targets of *UB3* in the regulation of tillering and panicle branching

To identify the DEGs that are directly regulated by *UB3*, we further analyzed RNA-seq data in depth by integrating with the
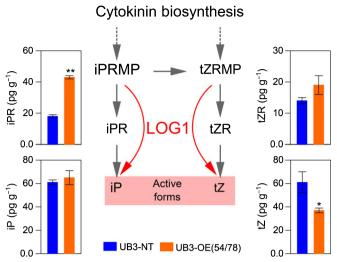
Cytokinin biosynthesis

Fig. 6 The comparison of the cytokinin biosynthesis pathway in rice nontransgenic plants (UB3-NT) and UB3-OE(54/78). The schematic represents the cytokinin biosynthesis pathway from iPRMP and tZRMP to the active cytokinin forms isopentenyladenine (iP) and trans-zeatin (tZ). The cytokinin content was measured in 60-d-old shoots of UB3-NT and UB3-OE(54/78) (with three biological replicates). iPRMP, N6-(D2-isopentenyl)adenine riboside monophosphate; tZRMP, trans-Zeatin riboside-5'-monophosphate. iPR, isopentenyladenine riboside; tZR, trans-zeatin riboside. *, $P < 0.05$; **, $P < 0.01$ (a Student's t-test). Values are means ± SD ($n = 3$).

ChIP-seq data reported by Lu *et al.* (Lu *et al.*, 2013). We found 115 (5.1%) DEGs in SAs and 151 (6.1%) DEGs in YPs that were shared with the ChIP-seq data (Fig. 4a; Table S6). Of these DEGs, 40 were differentially expressed in both SAs and YPs, and 28 of 40 DEGs contain the TGGGCC/T motif or the GTAC motif in their promoter regions, which indicated that these genes might be specifically bound by *OsSPL14* or its homologous gene *UB3 in vivo*. Among the 28 genes, two cytokinin biosynthesis-related genes, *LOG1* and *LOC_OS04G44354*, contain the SBP-box protein-binding GTAC motif in their promoter regions. Furthermore, we performed EMSAs to determine whether the UB3 protein binds to the promoters of these two genes directly *in vitro*. As shown in Fig. 5(a,b), GST-UB3 could significantly reduce the electrophoresis mobility of the probes containing the GTAC motif, while the mobility of the mutated probes carrying the GGAC motif was unaffected. Therefore, *UB3* could directly target the promoters of *LOG1* and *LOC_OS04G44354* and negatively regulate their expression. In addition, we identified the promoters of three genes involved in cytokinin signaling and degradation, including *OsRR1*, *OsRR6* and *OsCKX2*, and several TF genes, such as *RCN1*, *RCN4*, *SPL14*, and *SPL17*, also carry the GTAC motif and could be bound specifically by GST-UB3, indicating that *UB3* could directly target these genes to regulate cytokinin and signaling in SAs and YPs (Figs 5c–i, S1).

Regulatory pathway of *UB3* in maize

We assumed that *UB3* could regulate branching at the early stage of ear development in maize via a similar pathway to that in rice. To test this hypothesis, we sequenced the transcriptome in immature ears (5–8 mm) of the wild-type line (W22) and the *ub3::mum* mutant (a Mutator-mediated mutant with a W22 background) in maize, each with three biological replicates. In total, 8034 DEGs, including 3541 up-regulated and 4493 down-regulated genes, were identified ($P < 0.001$) in the *ub3::mum* (Fig. 7a; Table S7). Importantly, we also found that 17 genes involved in the cytokinin-O-glucoside biosynthesis were up-regulated, and three genes involved in cytokinin degradation were down-regulated in the *ub3::mum* mutant. We also analyzed the expression of genes involved in auxin biosynthesis and transport, and TF families, and found that 14 genes involved in auxin biosynthesis, nine genes in the *AP2* gene family, 16 genes in the *SPL* family and 20 genes in the *MADS-box* family were differentially expressed between W22 and the *ub3::mum* mutant (Fig. 7a; Table S7a–d). Furthermore, four representative genes – *GRMZM2G175910* (*GRM910*) encoding a cytokinin-O-glucosyltransferase, *GRMZM2G146688* encoding an AP2-EREBP-TF (*EREB41*), *GRMZM2G067624* encoding a squamosa promoter binding protein (*SBP29*) and *GRMZM2G046885* encoding a MADS-box TF (*MADS73*) – were selected for gel EMSA to determine whether the promoter of these genes could be bound directly by UB3 protein *in vitro*. The results showed that the promoter regions of all four genes could be specifically bound by GST-UB3 protein (Fig. 7b–e).

Furthermore, we focused on the genes that participated in *CLV-WUS* feedback loop in the maize meristems, including *td1*, *fea2, ct2* and *fea3*, and other classic genes like *FON2-LIKE CLE PROTEIN1* (*ZmFCP1*), *ZmWUS1* and *ZmCLV3*. RNA-seq and QRT-PCR showed that *fea2*, *ct2* and *fea3* were significantly down-regulated but *ZmFCP1*, *ZmWUS1 and ZmCLV3* were significantly up-regulated in the *ub3::mum* mutant (Fig. S3e; Table S7). EMSA assays showed that *UB3* could directly target the promoter regions of *ZmFCP1* and *ZmWUS1*, indicating that expressions of both *ZmFCP1* and *ZmWUS1* might be regulated by *UB3* directly (Figs 7f,g, S3e).

Discussion

The effects of *UB3* in the regulation of vegetative and reproductive branching

UB3 is an SBP-TF gene and negatively regulates maize KRN (Chuck *et al.*, 2014; Liu *et al.*, 2015). The *SBP/SPL* gene family modulates inflorescence development in *Arabidopsis* and rice (Chen *et al.*, 2010). During rice panicle development, *SPL7*, *SPL14* and *SPL17* have been shown to be highly expressed (Wang *et al.*, 2015). In this study, growth of the whole plant was dramatically suppressed, the transition from the vegetative to the reproductive phase was delayed, and plant height, tiller number, panicle branches and grain numbers per panicle were decreased in UB3-OE(54/78), compared with UB3-NT (Fig. 2; Table S3). These results indicate that the *SPL* family contributes to the transition from later panicle branches to the spikelet and negatively regulating the branching system. In addition, our results showed that the panicle size of UB3-OE(30) with moderate *UB3* expression was significantly larger, but its plant height and tiller
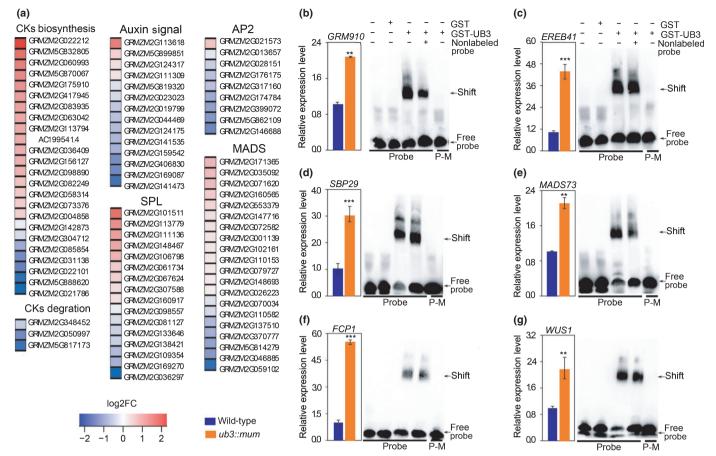
Fig. 7 Expression profiling of the *ub3::mum* mutant and wild-type in maize immature ear and gel electrophoretic mobility shift assay (EMSA) of putative *UB3* targets. (a) Differentially expressed genes (DEGs) in cytokinin biosynthesis and degradation pathway, auxin biosynthesis pathway, *AP2* gene family, *SPL* gene family and *MADS-box* gene family. The color in each cell indicates the value of the $\log_2$ fold-change ($\log_2$FC). All DEGs are listed in Supporting Information Table S7 ($P < 0.0001$). (b–g) The histogram in the box shows the expression level of genes in the *ub3::mum* mutant and wild-type, including (b) GRMZM2G175910, (c) EREB41-GRMZM2G146688, (d) SBP29-GRMZM2G067624, (e) MADS73-GRMZM2G046885, (f) FCP1-GRMZM2G165836 and (g) WUS1-GRMZM2G047448. Maize *ACTIN* (GRMZM2G126010) was used as the internal control. Values are means ± SE ($n = 3$). Primer sequences are listed in Table S1. *, $P < 0.05$; **, $P < 0.01$; ***, $P < 0.001$. The gel shift images show that UB3 protein could bind directly to the promoter regions of these genes containing two or three GTAC motifs. Probe, a 60 bp DNA containing the GTAC motif. P-M, the mutant probe with GCAC motif that can be used as a negative control. EMSA probe sequences are listed in Table S2.

number were slightly lower than that of UB3-NT (Fig. 2b–e,i–l; Table S3). QRT-PCR showed that *SPL7*, *SPL14* and *SPL17* were down-regulated in UB3-OE(54/78) but up-regulated in the moderate *UB3* expression line UB3-OE(30) (Fig. 3a,b). It has been reported that *miR156* and *miR529* modulate *SPL* levels to achieve an optimal panicle size (Wang *et al.*, 2015). We suggest that exogenous *UB3* can cooperate with other *SPL* genes in rice to ensure a modest expression level of *SPLs*, which then keep an appropriate number of panicle branches and grains per panicle.

UB3 regulates branching patterns by modulating the cytokinin pathway

Phytohormones, including cytokinin, IAA and SLs, are the main regulators of rice branching patterns. In particular, the accumulation of cytokinins in meristems is highly correlated with the branching pattern. The *LOG1* gene, encoding a cytokinin-activating enzyme that functions in the final step of bioactive cytokinin synthesis, is required to maintain meristem activity in

rice (Kurakawa *et al.*, 2007). The *An-2* gene, a homolog of *LOG*, enhances awn elongation by increasing the endogenous cytokinin concentration (Gu *et al.*, 2015). *Gn1a*, encoding a *CYTOKININ OXIDASE/DEHYDROGENASE* (*CKX*) *OsCKX2*, negatively regulates the cytokinin accumulation in inflorescence meristems (Ashikari *et al.*, 2005). Type A response regulators (*ARRs*) represent primary cytokinin-responsive genes in rice and *Arabidopsis*, acting as negative regulators of cytokinin-induced responses (To *et al.*, 2004; Jain *et al.*, 2006; Tsai *et al.*, 2012). In the present study, we found that the cytokinin level affected SAM size and activity and subsequently affected plant height, tillers and panicle branches (Figs 1, 2; Tables S3, S4). Our RNA-seq data revealed that many SAM differentiation-related genes, including genes participating in cytokinin biosynthesis and signaling, were down-regulated, such as *LOG1* in cytokinin biosynthesis and five A-type RR genes (*OsRR1*, *OsRR4*, *OsRR6*, *OsRR9* and *OsRR10*) in the cytokinin response pathway. However, *OsCKX2*, which functions in cytokinin degradation, was up-regulated by exogenous *UB3* (Fig. 5a–e, S1). These genes were highly expressed in SAs

and YPs, and they were significantly differentially expressed in at least one stage of development. EMSA showed that UB3 protein could directly bind to the GTAC motif in the promoter regions of these genes (Fig. 5a–e). Measurement of hormone concentrations showed that endogenous cytokinin levels were reduced in transgenic lines (Fig. 6). In summary, *UB3* directly targets and represses expression of cytokinin biosynthesis and signaling-related genes, and promotes expression of cytokinin degradation-related genes, resulting in lower cytokinin levels in SAs, which in turn inhibit the development of axillary buds when *UB3* is highly expressed in rice. We also analyzed the expression of these genes in YPs of UB3-OE(30) with moderate *UB3* expression: *LOG1* and *OsCKX2* showed insignificant change, and *RR4, RR6, RR9, RCN1* and *RCN4* were up-regulated relative to those in UB3-NT. The expression level of cytokinin synthesis and signaling-related genes in YPs might interpret the enlarged panicle size in UB3-OE(30) partly.

In addition to genes involved in cytokinin synthesis and signaling, many inflorescence-related TFs were differentially expressed between UB3-OE(54/78) and UB3-NT. In this study, we analysed the promoter region of TFs that are associated with inflorescence architecture and that also showed altered expression levels in rice, such as *SPL14, SPL17, RCN1* and *RCN4*. We found the *cis*-acting GTAC motif in these genes. Thus, we suggest that *UB3* can also regulate the expression levels of *SPL17, SPL14, RCN1* and *RCN4* in SAs and YPs by directly targeting the promoter regions to modulate tillering and branching.

Putative mechanism of *UB3* in maize

Both maize and rice are monocots that generate tillers and branches, and a similar hormone regulatory pathway is often expected to control branching in the two crop plants. In rice, genes in cytokinin or auxin signaling had been widely reported to regulate axillary bud and panicle development. In maize, however, cytokinin-related genes in the regulation of maize inflorescence architecture are still poorly understood. *aberrant phyllotaxy1* (*abph1*), encoding an A-type cytokinin response regulator, acts as a negative regulator of cytokinin signaling and a positive regulator of auxin concentration in determining SAM size, showing a crosstalk between cytokinin and auxin in maize (Lee *et al.*, 2009). In this study, *UB3* negatively regulated tillering and panicle branching in UB3-OE(54/78) with high *UB3* expression rice lines by reducing the active cytokinin level (Fig. 6). Similarly, in maize, RNA-seq data revealed that 17 cytokinin biosynthesis-related genes were up-regulated and three cytokinin degradation-related genes were down-regulated in the *ub3::mum* mutant (Fig. 7a). The result suggests that cytokinin level is possibly higher in the *ub3::mum* mutant than in the wild-type. The higher cytokinin level in the *ub3::mum* mutant probably promotes the lateral division of cells to initiate more primordia in meristems, which potentially develop into kernel rows. In addition to cytokinin-related genes, we also found that 10 out of 14 DEGs involved in auxin biosynthesis were down-regulated in the *ub3::mum* mutant (Fig. 7a). Therefore, the increased kernel rows

in the *ub3::mum* mutant ear may be a result of the crosstalk between cytokinin and auxin.

In addition, the *fea2, ct2* and *fea3 genes* in the *CLV-WUS* feedback loop were down-regulated but *ZmFCP1, ZmWUS1* and *ZmCLV3* were up-regulated in the *ub3::mum* mutant (Fig. S3e). And UB3 protein could directly target *ZmFCP1* and *ZmWUS1* (Fig. 7f,g). Previous studies suggested that *fea2* and *fea3* target to same downstream genes to transport *CLAVATA3/ESR*-related (*CLE*) signal from the leaf primordia, leading to wide expression of *ZmWUS1* and up-regulation of *CLV3* that directly correlates with fasciation (Brand *et al.*, 2000; Je *et al.*, 2016). Thus, we suggest that *UB3* regulates the development of kernel rows via regulation of *ZmFCP1* and *ZmWUS1* in the *CLV-WUS* pathway.

Author contributions

Z.Z. and Y.D. conceived and designed the experiments. Y.D., L.L., M.L., S.F., X.S. and J.C. performed the experiments. Y.D., L.L. and Z.Z. analyzed the data. Y.D. and Z.Z. wrote the paper.

References

Andrews S. 2010. *FastQC: a quality control tool for high-throughput sequence data.* [WWW document] URL http://www.bioinformatics.babraham.ac.uk/projects/fastqc.

Ashikari M, Sakakibara H, Lin S, Yamamoto T, Takashi T, Nishimura A, Angeles ER, Qian Q, Kitano H, Matsuoka M. 2005. Cytokinin oxidase regulates rice grain production. *Science* 5735: 741–745.

Bartlett ME, Williams SK, Taylor Z, DeBlasio S, Goldshmidt A, Hall DH, Schmidt RJ, Jackson DP, Whipple CJ. 2015. The maize *PI/GLO* ortholog *Zmm16/sterile tassel silky ear1* interacts with the zygomorphy and sex determination pathways in flower development. *Plant Cell* 11: 3081–3098.

Bommert P, Je BI, Goldshmidt A, Jackson D. 2013a. The maize *Gα* gene *COMPACT PLANT2* functions in *CLAVATA* signalling to control shoot meristem size. *Nature* 7472: 555–558.

Bommert P, Lunde C, Nardmann J, Vollbrecht E, Running M, Jackson D, Hake S, Werr W. 2005. *thick tassel dwarf1* encodes a putative maize ortholog of the *Arabidopsis CLAVATA1* leucine-rich repeat receptor-like kinase. *Development* 6: 1235–1245.

Bommert P, Nagasawa NS, Jackson D. 2013b. Quantitative variation in maize kernel row number is controlled by the *FASCIATED EAR2* locus. *Nature Genetics* 3: 334–337.

Brand U, Fletcher JC, Hobe M, Meyerowitz EM, Simon R. 2000. Dependence of stem cell fate in *Arabidopsis* on a feedback loop regulated by *CLV3* activity. *Science* 5479: 617–619.

Chen X, Zhang Z, Liu D, Zhang K, Li A, Mao L. 2010. *SQUAMOSA promoter-binding protein-like* transcription factors: star players for plant growth and development. *Journal of Integrative Plant Biology* 11: 946–951.

Chuck GS, Brown PJ, Meeley R, Hake S. 2014. Maize *SBP-box* transcription factors *unbranched2* and *unbranched3* affect yield traits by regulating the rate of lateral primordia initiation. *Proceedings of the National Academy of Sciences, USA* **52**: 18775–18880.

Chuck G, Cigan AM, Saeteurn K, Hake S. 2007a. The heterochronic maize mutant *Corngrass1* results from overexpression of a tandem microRNA. *Nature Genetics* **4**: 544–549.

Chuck G, Meeley R, Irish E, Sakai H, Hake S. 2007b. The maize *tasselseed4* microRNA controls sex determination and meristem cell fate by targeting *Tasselseed6/indeterminate spikelet1*. *Nature Genetics* **12**: 1517–1521.

Deshpande GM, Ramakrishna K, Chongloi GL, Vijayraghavan U. 2015. Functions for rice *RFL* in vegetative axillary meristem specification and outgrowth. *Journal of Experimental Botany* **66**: 2773–2784.

Eveland AL, Goldshmidt A, Pautler M, Morohashi K, Liseron-Monfils C, Lewis MW, Kumari S, Hiraga S, Yang F, Unger-Wallace E et al. 2014. Regulatory modules controlling maize inflorescence architecture. *Genome Research* **3**: 431–443.

Frame BR, Shou H, Chikwamba R, Zhang Z, Xiang C, Fonger T, Pegg S-E, Li B, Nettleton D, Pei P et al. 2002. Agrobacterium-mediated transformation of maize embryos using a standard binary vector system. *Plant Physiology* **129**: 13–22.

Galli M, Liu Q, Moss BL, Malcomber S, Li W, Gaines C, Federici S, Roshkovan J, Meeley R, Nemhauser JL et al. 2015. Auxin signaling modules regulate maize inflorescence architecture. *Proceedings of the National Academy of Sciences, USA* **43**: 13372–13377.

Goecks J, Nekrutenko A, Taylor J, Galaxy Team. 2010. Galaxy: a comprehensive approach for supporting accessible, reproducible, and transparent computational research in the life sciences. *Genome Biology* **11**: R86.

Gomez-Roldan V, Fermas S, Brewer PB, Puech-Pagès V, Dun EA, Pillot JP, Letisse F, Matusova R, Danoun S, Portais JC et al. 2008. Strigolactone inhibition of shoot branching. *Nature* **455**: 189–194.

Gu B, Zhou T, Luo J, Liu H, Wang Y, Shangguan Y, Zhu J, Li Y, Sang T, Wang Z et al. 2015. *An-2* encodes a cytokinin synthesis enzyme that regulates awn length and grain production in rice. *Molecular Plant* **11**: 1635–1650.

Ha CM, Jun JH, Fletcher JC. 2010. Shoot apical meristem form and function. *Current Topics in Developmental Biology* **91**: 103–140.

Hu Y, Liang W, Yin C, Yang X, Ping B, Li A, Jia R, Chen M, Luo Z, Cai Q et al. 2015. Interactions of *OsMADS1* with floral homeotic genes in rice flower development. *Molecular Plant* **9**: 1366–1384.

Jain M, Tyagi AK, Khurana JP. 2006. Molecular characterization and differential expression of cytokinin-responsive type-A response regulators in rice (*Oryza sativa*). *BMC Plant Biology* **6**: 1.

Je BI, Gruel J, Lee YK, Bommert P, Arevalo ED, Eveland AL, Wu Q, Goldshmidt A, Meeley R, Bartlett M et al. 2016. Signaling from maize organ primordia via *FASCIATED EAR3* regulates stem cell proliferation and yield traits. *Nature Genetics* **48**: 785–791.

Jiao Y, Wang Y, Xue D, Wang J, Yan M, Liu G, Dong G, Zeng D, Lu Z, Zhu X et al. 2010. Regulation of *OsSPL14* by *OsmiR156* defines ideal plant architecture in rice. *Nature Genetics* **6**: 541–544.

Kant S, Bi YM, Zhu T, Rothstein SJ. 2009. *SAUR39*, a small auxin-up RNA gene, acts as a negative regulator of auxin synthesis and transport in rice. *Plant Physiology* **151**: 691–701.

Kurakawa T, Ueda N, Maekawa M, Kobayashi K, Kojima M, Nagato Y, Sakakibara H, Kyozuka J. 2007. Direct control of shoot meristem activity by a cytokinin-activating enzyme. *Nature* **7128**: 652–655.

Lee BH, Johnston R, Yang Y, Gallavotti A, Kojima M, Travençolo BA, Costa Lda F, Sakakibara H, Jackson D. 2009. Studies of *aberrant phyllotaxy1* mutants of maize indicate complex interactions between auxin and cytokinin signaling in the shoot apical meristem. *Plant Physiology* **1**: 205–216.

Liu L, Du Y, Shen X, Li M, Sun W, Huang J, Liu Z, Tao Y, Zheng Y, Yan J et al. 2015. *KRN4* controls quantitative variation in maize kernel row number. *PLoS Genetics* **11**: e1005670.

Lu G, Coneva V, Casaretto JA, Ying S, Mahmood K, Liu F, Nambara E, Bi YM, Rothstein SJ. 2015. *OsPIN5b* modulates rice (*Oryza sativa*) plant architecture and yield by changing auxin homeostasis, transport and distribution. *Plant Journal* **83**: 913–925.

Lu Z, Yu H, Xiong G, Wang J, Jiao Y, Liu G, Jing Y, Meng X, Hu X, Qian Q et al. 2013. Genome-wide binding analysis of the transcription activator *ideal plant architecture1* reveals a complex network regulating rice plant architecture. *Plant Cell* **10**: 3743–3759.

Miura K, Ikeda M, Matsubara A, Song XJ, Ito M, Asano K, Matsuoka M, Kitano H, Ashikari M. 2010. *OsSPL14* promotes panicle branching and higher grain productivity in rice. *Nature Genetics* **6**: 545–549.

Mortazavi A, Williams BA, McCue K, Schaeffer L, Wold B. 2008. Mapping and quantifying mammalian transcriptomes by RNA-Seq. *Nature Methods* **5**: 621–628.

Müller D, Leyser O. 2011. Auxin, cytokinin and the control of shoot branching. *Annals of Botany* **107**: 1203–1212.

Ohmori Y, Tanaka W, Kojima M, Sakakibara H, Hirano HY. 2013. *WUSCHEL-RELATED HOMEOBOX4* is involved in meristem maintenance and is negatively regulated by the *CLE* gene *FCP1* in rice. *Plant Cell* **25**: 229–241.

Pautler M, Eveland AL, LaRue T, Yang F, Weeks R, Lunde C, Je B, Meeley R, Komatsu M, Vollbrecht E et al. 2015. *FASCIATED EAR4* encodes a bZIP transcription factor that regulates shoot meristem size in maize. *Plant Cell* **1**: 104–120.

Pautler M, Tanaka W, Hirano HY, Jackson D. 2013. Grass meristems I: shoot apical meristem maintenance, axillary meristem determinacy and the floral transition. *Plant and Cell Physiology* **54**: 302–312.

Studer A, Zhao Q, Ross-Ibarra J, Doebley J. 2011. Identification of a functional transposon insertion in the maize domestication gene *tb1*. *Nature Genetics* **11**: 1160–1163.

Suzuki T, Ohneda M, Toriba T, Yoshida A, Hirano HY. 2009. *FON2 SPARE1* redundantly regulates floral meristem maintenance with *FLORAL ORGAN NUMBER2* in rice. *PLoS Genetics* **10**: e1000693.

Suzuki T, Sato M, Ashikari M, Miyoshi M, Nagato Y, Hirano HY. 2004. The gene *FLORAL ORGAN NUMBER1* regulates floral meristem size in rice and encodes a leucine-rich repeat receptor kinase orthologous to Arabidopsis *CLAVATA1*. *Development* **22**: 5649–5657.

Suzuki T, Toriba T, Fujimoto M, Tsutsumi N, Kitano H, Hirano HY. 2006. Conservation and diversification of meristem maintenance mechanism in *Oryza sativa*: function of the *FLORAL ORGAN NUMBER2* gene. *Plant and Cell Physiology* **12**: 1591–1602.

Suzuki T, Yoshida A, Hirano HY. 2008. Functional diversification of *CLAVATA3*-related CLE proteins in meristem maintenance in rice. *Plant Cell* **8**: 2049–2058.

Tanaka W, Ohmori Y, Ushijima T, Matsusaka H, Matsushita T, Kumamaru T, Kawano S, Hirano HY. 2015. Axillary meristem formation in rice requires the *WUSCHEL* Ortholog *TILLERS ABSENT1*. *Plant Cell* **4**: 1173–1184.

Tanaka W, Pautler M, Jackson D, Hirano HY. 2013. Grass meristems II: inflorescence architecture, flower development and meristem fate. *Plant and Cell Physiology* **3**: 313–324.

To JP, Haberer G, Ferreira FJ, Deruère J, Mason MG, Schaller GE, Alonso JM, Ecker JR, Kieber JJ. 2004. Type-A *Arabidopsis* response regulators are partially redundant negative regulators of cytokinin signaling. *Plant Cell* **3**: 658–671.

Trapnell C, Roberts A, Goff L, Pertea G, Kim D, Kelley DR, Pimentel H, Salzberg SL, Rinn JL, Pachter L. 2012. Differential gene and transcript expression analysis of RNA-seq experiments with TopHat and Cufflinks. *Nature Protocols* **7**: 562–578.

Tsai YC, Weir NR, Hill K, Zhang W, Kim HJ, Shiu SH, Schaller GE, Kieber JJ. 2012. Characterization of genes involved in cytokinin signaling and metabolism from rice. *Plant Physiology* **4**: 1666–1684.

Tsuda K, Ito Y, Sato Y, Kurata N. 2011. Positive autoregulation of a *KNOX* gene is essential for shoot apical meristem maintenance in rice. *Plant Cell* **12**: 4368–4381.

Tsuda K, Kurata N, Ohyanagi H, Hake S. 2014. Genome-wide study of *KNOX* regulatory network reveals brassinosteroid catabolic genes important for shoot meristem function in rice. *Plant Cell* **9**: 3488–3500.

Vollbrecht E, Schmidt RJ. 2009. Handbook of maize. In: Bennetzen JL, Hake S, eds. *Development of the inflorescences*. New York, USA: Springer, 13–40.

Wang L, Sun S, Jin J, Fu D, Yang X, Weng X, Xu C, Li X, Xiao J, Zhang Q. 2015. Coordinated regulation of vegetative and reproductive branching in rice. *Proceedings of the National Academy of Sciences, USA* **50**: 15504–15509.

Zheng M, Wang Y, Wang C, Ren Y, Lv J, Peng C, Wu T, Liu K, Zhao S, Liu X
et al. 2015. *DEFORMED FLORAL ORGAN1* (*DFO1*) regulates floral organ
identity by epigenetically repressing the expression of *OsMADS58* in rice
(*Oryza sativa*). *New Phytologist* 4: 1476–1490.

Zhu QH, Hoque MS, Dennis ES, Upadhyaya NM. 2003. Ds tagging of
BRANCHED FLORETLESS 1 (*BFL1*) that mediates the transition from
spikelet to floret meristem in rice (*Oryza sativa* L). *BMC Plant Biology* 3: 1–6.

Supporting Information

Additional Supporting Information may be found online in the
Supporting Information tab for this article:

Fig. S1. Quantitative real-time PCR validation of 20 differentially expressed genes in rice young panicles.

Fig. S2. Quantitative real-time PCR validation of differentially expressed genes involved in auxin biosynthesis in rice and IAA content in rice shoots.

Fig. S3. Quantitative real-time PCR validation of 32 differentially expressed genes, including *AP2* family, *SPL* family, *MADS* family and genes associated with meristem size in the *ub3::mum* mutant and wild-type.

Table S1. Primers used for vector construction, identification, and quantitative real-time PCR in rice and maize

Table S2. Probes used in the electrophoretic mobility shift assay

Table S3 Performance of agronomic traits in *UB3* overexpression lines and nontransgenic plants (UB3-NT) in rice

Table S4 Growth rate of plant height and tillers per plant in *UB3* overexpression lines and nontransgenic plants (UB3-NT) in rice

Table S5 Differentially expressed genes between UB3-OE(54/78) and nontransgenic plants (UB3-NT) in the shoot apicals and young panicles of rice

Table S6 Genes shared by differentially expressed genes and genes detected by *IPA1* ChIP-seq in a previous study

Table S7 Differentially expressed genes between the *ub3::mum* mutant and wild-type in maize immature ear

Please note: Wiley Blackwell are not responsible for the content or functionality of any Supporting Information supplied by the authors. Any queries (other than missing material) should be directed to the *New Phytologist* Central Office.